GENERALIZED AUTOCORRELATION ANALYSIS FOR MULTI-TARGET DETECTION

*Ye'Ela Shalit**, Ran Weber**, Asaf Abas†*, Shay Kreymer**, and Tamir Bendory**

*School of Electrical Engineering, Tel Aviv University, Tel Aviv, Israel
†Department of Applied Mathematics, Tel Aviv University, Tel Aviv, Israel

ABSTRACT

We study the multi-target detection (MTD) problem of recovering a target signal from a noisy measurement that contains multiple copies of the signal at unknown locations. Motivated by the structure reconstruction problem in single-particle cryo-electron microscopy, we focus on the high noise regime, where the noise hampers accurate detection of signal occurrences. Previous works on the MTD model proposed an autocorrelation analysis framework, where the goal is finding a signal that best matches the observable autocorrelations by minimizing a least squares objective. This allows estimating the signal directly from the measurement, circumventing estimating the unknown locations. This paper extends this line of research by developing a generalized autocorrelation analysis framework that replaces the least squares by a weighted least squares. The optimal weights can be computed directly from the data and guarantee favorable statistical properties. We demonstrate signal recovery from highly noisy measurements, and show that the proposed framework outperforms classical autocorrelation analysis in a wide range of parameters.

***Index Terms*—** Autocorrelation analysis, generalized method of moments, multi-target detection, single-particle cryo-electron microscopy.

1. INTRODUCTION

We study the multi-target detection (MTD) problem of estimating a target signal $x \in \mathbb{R}^L$ from a noisy measurement that contains multiple copies of the signal, each randomly translated [1], [2], [3], [4], [5], [6]. Specifically, let $y \in \mathbb{R}^N$ be a measurement of the form

$$y[\ell] = \sum_{i=1}^{p} x[\ell - \ell_i] + \varepsilon[\ell], \tag{1}$$

where $\{\ell_i\}_{i=1}^p \in \{L+1, \dots, N-L\}$ are translations, $L \ll N$, and $\varepsilon[\ell] \overset{\text{i.i.d.}}{\sim} \mathcal{N}(0, \sigma^2)$. The translations and the number of occurrences of x in y, denoted by p, are unknown. We assume that the signal occurrences are sufficiently separated from each other. Specifically, each occurrence of x in the measurement y is separated by at least a full signal length from its neighbors, namely,

$$|\ell_{i_1} - \ell_{i_2}| \geq 2L - 1, \quad \text{for all } i_1 \neq i_2. \tag{2}$$

This model is referred to as the well-separated model [1]. Figure 1 presents an example of three possible measurements y at different signal-to-noise ratios (SNRs). We define SNR $:= \frac{\|x\|_2^2}{L\sigma^2}$.

The MTD model serves as a mathematical abstraction of the cryo-electron microscopy (cryo-EM) technology for macromolecular structure determination [7], [8], [9]. In a cryo-EM experiment [10], biological macromolecules suspended in a liquid solution are rapidly frozen into a thin ice layer. An electron beam then passes through the sample, and a two-dimensional tomographic projection is recorded. Importantly, the 2-D location and 3-D orientation of particles within the ice are random and unknown. This measurement is further affected by high noise levels and the optical configuration of the microscope.

In the current analysis workflow of cryo-EM data [11], [12] [13], [14], the 2-D projections are first detected and extracted from the micrograph, and later rotationally and translationally aligned to reconstruct the 3-D molecular structure. This approach fails for small molecules, which induce low contrast, and thus low SNR. This makes them difficult to detect and align [6], [12] [7], [15], rendering current cryo-EM algorithmic pipeline ineffective. For example, in the limit SNR $\to 0$, reliable detection of signals' locations within the measurement is impossible [6, Proposition 3.1].

The MTD model was devised in [6] in order to study the recovery of small molecules directly from the micrograph, below the current detection limit of cryo-EM [7], [16]. An autocorrelation analysis technique (see Section 2.1) was implemented to recover low-resolution 3-D structures from noiseless simulated data under a simplified model. In order to further investigate the method from analytical and computational perspectives, the MTD model was studied in [1] for one-dimensional signals and under the assumption that the signal occurrences are either well-separated (as in this paper) or follow a Poisson distribution. In [2], the mathematical framework was extended to account for arbitrary spacing of one-dimensional signal occurrences. In [3], [4], the authors studied the MTD problem in two dimensions, where the sought images are arbitrarily rotated, but still well-separated, and in [5] the framework was extended to account for an arbitrary spacing distribution of image occurrences.

Autocorrelation analysis is a special case of the method of moments, a classical statistical inference technique, and was first proposed for cryo-EM data in [17]; see also [18], [19], [20]. It consists of finding a signal that best matches the empirical autocorrelations of the measurement, usually by minimizing a least-squares (LS) objective (see Section 2.1). For any noise level, the empirical autocorrelations can be estimated to any desired accuracy for sufficiently large N. Computing the autocorrelations is straightforward and requires only one pass over the data, which is advantageous for massively large datasets, such as cryo-EM datasets [11]. This work studies the application of a *generalized autocorrelation analysis* to the MTD problem. The generalized autocorrelation analysis framework, which is a special case of the generalized method of moments (GMM) [21], suggests replacing the LS objective of autocorrelation analysis with a weighted LS, and provides a recipe of how to compute the optimal weights; see Section 2.2. GMM has been proven

* These four authors have contributed equally to this work.

S.K. is supported by the Yitzhak and Chaya Weinstein Research Institute for Signal Processing. T.B. is supported in part by NSF-BSF grant no. 2019752.

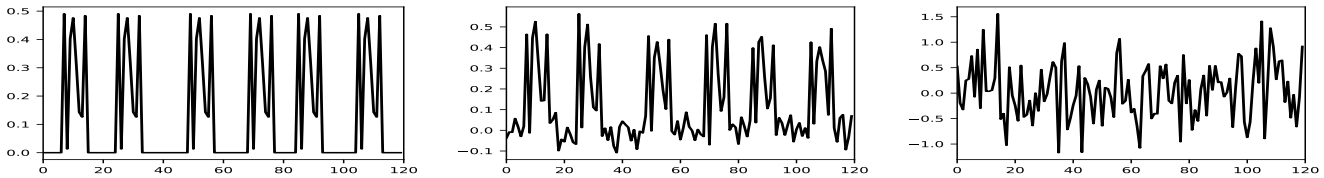

(a) No noise (b) SNR $= 50$ (c) SNR $= 0.5$

Fig. 1: Three MTD measurements (1) of length $N = 120$ at different noise levels: (a) no noise; (b) SNR $= 50$; (c) SNR $= 0.5$. Each measurement contains six copies of the target signal. Our goal is to estimate the target signal directly from y. We focus on the low SNR regime (e.g., panel (c)) in which the signal occurrences are swamped by the noise, and the locations of the signal occurrences cannot be reliably detected.

to be highly effective in a variety of computational tasks, see for example [22], [23], [24], [25], [26]. We mention in passing that the framework can be formulated with other objective functions, rather than LS [27].

The main contribution of this paper is extending the autocorrelation analysis framework introduced in [1] by developing a generalized autocorrelation analysis framework for the MTD problem. We devise an algorithm for recovering the target signal from a measurement, and demonstrate successful reconstructions in noisy regimes (see Section 3). Moreover, we show that the generalized autocorrelation analysis estimator outperforms the classical autocorrelation analysis estimator in a wide range of SNRs and measurement's lengths. It is thus a first step towards applying a generalized autocorrelation analysis to recovering small molecules from cryo-EM experimental datasets [6].

2. COMPUTATIONAL FRAMEWORK

2.1. Autocorrelation analysis

Before introducing the generalized autocorrelation analysis framework, we begin by presenting a classical autocorrelation analysis. The autocorrelation of order q of a signal $z \in \mathbb{R}^N$ is defined as

$$A_z^q[\ell_1, \ldots, \ell_{q-1}] := \mathbb{E}_z\Big[\frac{1}{N}\sum_{i\in\mathbb{Z}} z[i]z[i+\ell_1]\cdots z[i+\ell_{q-1}]\Big], \quad (3)$$

where $\ell_1, \ldots, \ell_{q-1}$ are integer shifts. Indexing out of bounds is zero-padded, that is, $z[i] = 0$ out of the range $\{0, \ldots, N-1\}$. As N grows indefinitely, by the law of large numbers the empirical autocorrelations of z almost surely (a.s.) converge to the population autocorrelations of z:

$$\lim_{N\to\infty} \frac{1}{N}\sum_{i\in\mathbb{Z}} z[i]z[i+\ell_1]\cdots z[i+\ell_{q-1}] \overset{\text{a.s.}}{=} A_z^q[\ell_1, \ldots, \ell_{q-1}]. \quad (4)$$

To formulate an autocorrelation analysis, we write the first three autocorrelation of y. We use the first three autocorrelations since the third-order autocorrelation is the lowest-order autocorrelation that determines a generic signal uniquely [1]. According to (4), the first-order autocorrelation is defined as

$$A_y^1 := \frac{1}{N}\sum_{i\in\mathbb{Z}} y[i], \quad (5)$$

which is just the mean of the measurement. The second-order autocorrelation of y, $A_y^2 : \mathbb{Z} \to \mathbb{R}$, is defined by

$$A_y^2[\ell_1] := \frac{1}{N}\sum_{i\in\mathbb{Z}} y[i]y[i+\ell_1]. \quad (6)$$

For almost all 1-D signals, the second-order autocorrelation does not contain enough information to determine a signal uniquely [28], [29]. The third-order autocorrelation $A_y^3 : \mathbb{Z}\times\mathbb{Z} \to \mathbb{R}$ is given by

$$A_y^3[\ell_1, \ell_2] := \frac{1}{N}\sum_{i\in\mathbb{Z}} y[i]y[i+\ell_1]y[i+\ell_2]. \quad (7)$$

Next, we want to relate those observable autocorrelations A_y^1, A_y^2, and A_y^3, to the signal x under the statistical model (1). Importantly, under the well-separated case (2), for shifts in the range $\mathcal{L} = \{0, \ldots, L-1\}$, any given occurrence of x in y is only ever correlated with itself, and never with another occurrence. In [1], it was shown that under the well-separated condition (2), for any fixed level of noise σ^2, density γ and signal length L, in the limit $N \to \infty$, the autocorrelations of the measurements are equal, possibly up to some predicted bias terms, to the autocorrelations of the signal times a density constant. Specifically, we have that

$$A_y^1 \overset{\text{a.s.}}{=} \gamma A_x^1, \quad (8)$$

$$A_y^2[\ell_1] \overset{\text{a.s.}}{=} \gamma A_x^2[\ell_1] + \sigma^2\delta[\ell_1], \quad (9)$$

$$A_y^3[\ell_1, \ell_2] \overset{\text{a.s.}}{=} \gamma A_x^3[\ell_1, \ell_2] + \gamma A_x^1 B(\ell_1, \ell_2), \quad (10)$$

for $\ell_1, \ell_2 \in \mathcal{L}$, where $B(x, \ell_1, \ell_2) := \sigma^2(\delta[\ell_1] + \delta[\ell_2] + \delta[\ell_1 - \ell_2])$, and $\delta[\ell] = \begin{cases} 1 \text{ if } \ell = 0, \\ 0 \text{ otherwise,} \end{cases}$ is the Kronecker delta function. Here, γ is the density of the target images in the measurement and is defined by

$$\gamma = p\frac{L}{N}. \quad (11)$$

For instance, the measurements in Figure 1 correspond to $\gamma = 0.4$. We note that if the signal occurrences violate the separation condition (2) but follow a Poisson distribution, the autocorrelations are equivalent to (8) - (10) [1].

Notably, the relations between the autocorrelations of y and x do not directly depend on the location of individual signal occurrences in the measurement, but only through the density parameter γ. Therefore, detecting the signal occurrences is not a prerequisite for signal recovery, and thus signal recovery is possible even in very low SNR regimes.

In [1], [2], [3], [4], [5], it was suggested to find the signal that best fits the observable autocorrelations by minimizing an LS objec-

tive. Specifically, using (8) - (10) the LS reads

$$\begin{aligned}&\min_{x,\gamma>0}(A_y^1-\gamma A_x^1)^2\\&+w_2\sum_{\ell_1=0}^{L-1}\|A_y^2[\ell_1]-\gamma A_x^2[\ell_1]-\sigma^2\delta[\ell_1]\|_2^2\\&+w_3\sum_{\ell_1=0}^{L-1}\sum_{\ell_2=0}^{L-1}\|A_y^3[\ell_1,\ell_2]-\gamma A_x^3[\ell_1,\ell_2]-\gamma A_x^1 B(\ell_1,\ell_2)\|_2^2,\end{aligned} \tag{12}$$

where the weights w_1, w_2, and w_3 were chosen such that each term is equally weighted, as suggested by [1]. We note that the optimization problem is non-convex, and thus there is no guarantee to converge to a global optimum. Nevertheless, similarly to previous papers on MTD, our numerical results (see Section 3) suggest that standard gradient-based methods succeed in recovering x from only a few random initial guesses.

2.2. Generalized autocorrelation analysis

The generalized autocorrelation analysis framework is a special case of the GMM. In its most simplified form, the GMM generalizes the method of moments by replacing the LS objective function with specific optimal weights. This choice guarantees favorable asymptotic statistical properties, such as the minimal asymptotic variance of the estimation error [21] (see Section 2.3). In this work, we adapt the GMM to autocorrelation analysis and term the method generalized autocorrelation analysis.

Let us define the moment function $f(\theta,y)\colon \Theta\times\mathbb{R}^r\to\mathbb{R}^q$, where Θ is a compact parameter space. The moment function is chosen such that its expectation is zero only at a single point $\theta=\theta_0$, where θ_0 is the ground truth parameters (in our case, the target signal x and the density parameter γ). Namely,

$$\mathbb{E}\left[f(\theta,y)\right]=0 \quad \text{if and only if} \quad \theta=\theta_0. \tag{13}$$

Since the moment function need only to satisfy the uniqueness condition (13) and a few additional mild regularity conditions (which can be found in [21] [30] [26]), the GMM was applied to a wide range of estimation problems, such as panel data problem [31] and subspace estimation [24].

In order to define the moment function for the MTD problem, we first define the i-th observation from the measurement y as follows:

$$y_i := [y[i],\ldots,y[i+L]]. \tag{14}$$

The natural choice of a moment function $f(\theta,y_i)$, for y_i from (14), is the discrepancy between the autocorrelations of y_i and the population autocorrelations:

$$f(\theta,y_i):=\begin{bmatrix}\gamma A_x^1-A_{y_i}^1\\ \left\{\gamma A_x^2[\ell_1]+\sigma^2\delta[\ell_1]-A_{y_i}^2[\ell_1]\right\}_{\ell_1=0}^{L-1}\\ \left\{\gamma A_x^3[\ell_1,\ell_2]+\gamma A_x^1 B(x,\ell_1,\ell_2)-A_{y_i}^3[\ell_1,\ell_2]\right\}_{\ell_1,\ell_2=0}^{L-1}\end{bmatrix}, \tag{15}$$

where $\theta:=[x,\gamma]$. Notice that the chosen moment function (15) fulfills the uniqueness condition (13) for a generic signal. The estimated sample moment function is the average of f over N observations:

$$g_N(\theta)=\frac{1}{N}\sum_{i=0}^{N-1}f(\theta,y_i). \tag{16}$$

The GMM estimator is defined as the minimizer of the weighted LS expression

$$\hat{\theta}_N=\arg\min_{\theta\in\Theta}\ g_N(\theta)^T W_N g_N(\theta). \tag{17}$$

Here, W_N is a fixed positive semi-definite (PSD) matrix. Note that the LS estimator (12) is a special case of (**??**), where W_N is the diagonal matrix with the weights from (12).

2.3. Large sample properties

Before presenting the statistical properties of the generalized autocorrelation analysis, we fix notation. We denote by $\xrightarrow{p}$ and $\xrightarrow{d}$ convergence in probability and in distribution, respectively. Let

$$S:=\lim_{N\to\infty}\operatorname{Cov}\left[\sqrt{N}g_N(\theta_0)\right], \tag{18}$$

be the covariance matrix of the estimated sample moment function (16) at the ground truth θ_0. We denote by $\{W_N\}_{N=1}^{\infty}$ a sequence of PSD matrices which converges almost surely to a positive definite matrix W. The expectation of the Jacobian of the moment function at the ground truth θ_0 is denoted by $G_0=\mathbb{E}\left[\partial f(\theta_0,y)/\partial\theta^T\right]$.

The large sample properties of the GMM estimator, and thus also of the generalized autocorrelation estimator, were derived in [21], and are presented in the following theorem. The regularity conditions for this theorem can be found in [21], [30], [26].

Theorem 2.1. *Under condition (13) and a few additional mild regularity conditions that can be found in [21], [30], [26], the GMM estimator (and thus also the generalized autocorrelation analysis estimator) satisfies:*

A. (Consistency) $\hat{\theta}_N\xrightarrow{p}\theta_0$.

B. (Asymptotic normality)

$$\sqrt{N}(\hat{\theta}_N-\theta_0)\xrightarrow{d}\mathcal{N}(0,MSM^T),$$

where $M=[G_0^T W G_0]^{-1}G_0^T W$.

C. (Optimal choice of a weighting matrix) *The minimum asymptotic variance of* $\hat{\theta}_N$ *is given by* $(G_0^T S^{-1}G_0)^{-1}$ *and is attained by* $W=S^{-1}$.

Theorem 2.1 shows that the matrix $W=S^{-1}$ guarantees a minimal asymptotic variance of the estimator's error. The covariance matrix S of (18), which plays a central role in Theorem 2.1, is required to be a positive definite matrix. Therefore, the moment function must be chosen so that S is full-rank. Empirically, in our case the matrix S is indeed full-rank after we remove repeating entries of f that appear due to the inherent symmetries of the autocorrelations [26]. We note that in general the matrix W depends on the ground truth θ_0, and thus cannot be computed from the data. Therefore, it is common to use iterative methods that alternate between optimizing (17) given W, and computing W given the current estimate of θ. However, for our specific choice of moment function (15), the matrix S is independent of the parameters of interest, and thus can be computed by

$$\operatorname{Cov}[g(\theta)]=\operatorname{Cov}\left[\left\{\left[A_{y_i}^1;\left\{A_{y_i}^2[\ell_1]\right\}_{\ell_1=0}^{L-1};\left\{A_{y_i}^3[\ell_1,\ell_2]\right\}_{\ell_1,\ell_2=0}^{L-1}\right]\right\}_{i=0}^{N-1}\right]. \tag{19}$$

Namely, the optimal weighting matrix can be computed using a single pass over the data.

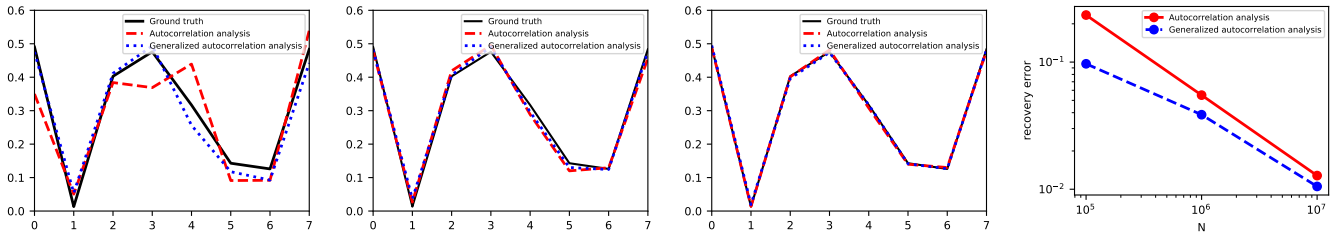

(a) $N = 10^5$ (b) $N = 10^6$ (c) $N = 10^7$ (d) Recovery error

Fig. 2: Panels (a), (b), and (c) present signal estimates using autocorrelation analysis (in red) and generalized autocorrelation analysis (in blue) with different measurement lengths. Panel (d) presents the recovery error using both methods, as a function of measurement length (N).

3. NUMERICAL EXPERIMENTS

This section compares the numerical performance of the generalized autocorrelation analysis framework and the classical autocorrelation analysis method. A comparison of autocorrelation analysis to a naive method that detects and extracts the signal occurrences, and then averages, was conducted in [2], [5]. While this method works well in a high SNR environment, it fails in low SNR regimes—the focal point of this paper—and thus omitted. The optimization problem (12) was minimized using the Broyden-Fletcher-Goldfarb-Shanno (BFGS) algorithm, while ignoring the positivity constraint on γ (namely, treating it as an unconstrained problem). We measure the estimation error by

$$\text{error}(x) = \frac{\|x - x^*\|_2}{\|x^*\|_2},$$

where x^* is the true signal, and x is the estimated signal. In the experiments presented in Sections 3.2 and 3.3, the measurements were generated according to (1) with density $\gamma = 0.2$, and the target signals are of length $L = 21$. Each entry of the signals was drawn i.i.d from a uniform distribution in $[0, 1]$, and the target signals were normalized such that $\|x\|_2 = 1$. We estimated the signal from 5 random initial guesses that were generated similarly to the ground truth signal and from $\gamma_{\text{init}} = 0.18$, and calculated the estimation error of the signal estimate whose final objective function is minimal. Figures 3 and 4 present the median error over 50 trials. The code to reproduce all experiments is publicly available at `https://github.com/krshay/MTD-GMM`.

3.1. Recovery from a noisy measurement

In Figure 2 we present a successful recovery of a target signal of length $L = 8$ from a noisy measurement with SNR $= 0.5$ and $\gamma = 0.2$, using autocorrelation analysis and generalized autocorrelation analysis. The noise level is visualized in Figure 1. As expected, the recovery error decreases as the measurement's length increases. Remarkably, for all measurement lengths N, the generalized autocorrelation analysis framework shows superior numerical performance.

3.2. Recovery error as a function of the measurement length

Figure 3 presents recovery error as a function of the measurement length N. We set SNR $= 50$, demonstrating a high SNR environment. As expected from the law of large numbers, the recovery error of both estimators decays as $N^{-1/2}$. Evidently, the generalized autocorrelation analysis estimator significantly outperforms the classical autocorrelation analysis estimator for all N.

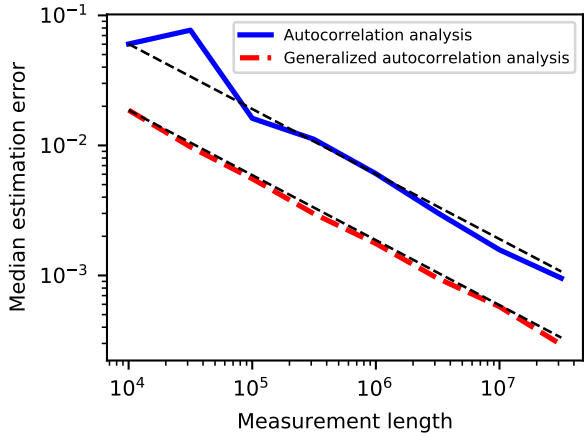

Fig. 3: The median estimation error as a function of the measurement length N with SNR $= 50$, by: (a) the autocorrelation analysis estimator; (b) the generalized autocorrelation analysis estimator. The black dashed lines illustrates a slope of $-1/2$, as predicted by the law of large numbers.

3.3. Recovery error as a function of the SNR

Figure 4 presents recovery error as a function of the SNR, for a fixed measurement length $N = 10^6$. For all levels of SNR, the recovery error using generalized autocorrelation analysis is smaller than the error using the standard autocorrelation analysis. In addition, the slope of the error curve increases dramatically at low SNR, around SNR ≈ 1, which is a known phenomenon in the cryo-EM literature, see for example [32], [33], [34].

4. CONCLUSION

This paper is motivated by the effort of reconstructing small 3-D molecular structures using cryo-EM, below the current detection limit. The main contribution of this study is incorporating the generalized method of moments into the computational framework proposed in [6] for the MTD problem. Theorem 2.1 shows the optimality of the framework, and it is corroborated by numerical experiments.

Future work includes extending the generalized autocorrelation analysis estimator to the 2-D and 3-D cases of the MTD problem [6]. Furthermore, we wish to extend the framework to the case of an

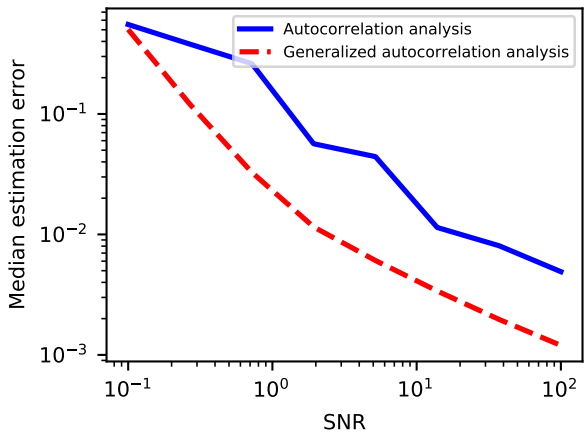

Fig. 4: The median estimation error as a function of SNR, for measurements with length $N = 10^6$, by: (a) the autocorrelation analysis estimator; (b) the generalized autocorrelation analysis estimator. Evidently, the generalized autocorrelation analysis estimator outperforms classical autocorrelation analysis for all SNR levels.

arbitrary spacing distribution between signal occurrences (namely, signals that violate the separation condition (2)) [2], [5], with the ultimate goal of applying the method to 3-D cryo-EM experimental datasets.

5. REFERENCES

[1] Tamir Bendory, Nicolas Boumal, William Leeb, Eitan Levin, and Amit Singer, "Multi-target detection with application to cryo-electron microscopy," *Inverse Problems*, vol. 35, no. 10, pp. 104003, 2019.

[2] Ti-Yen Lan, Tamir Bendory, Nicolas Boumal, and Amit Singer, "Multi-target detection with an arbitrary spacing distribution," *IEEE Transactions on Signal Processing*, vol. 68, pp. 1589–1601, 2020.

[3] Nicholas F Marshall, Ti-Yen Lan, Tamir Bendory, and Amit Singer, "Image recovery from rotational and translational invariants," in *ICASSP 2020-2020 IEEE International Conference on Acoustics, Speech and Signal Processing (ICASSP)*. IEEE, 2020, pp. 5780–5784.

[4] Tamir Bendory, Ti-Yen Lan, Nicholas F Marshall, Iris Rukshin, and Amit Singer, "Multi-target detection with rotations," *arXiv preprint arXiv:2101.07709*, 2021.

[5] Shay Kreymer and Tamir Bendory, "Two-dimensional multi-target detection: an autocorrelation analysis approach," *arXiv preprint arXiv:2105.06765*, 2021.

[6] Tamir Bendory, Nicolas Boumal, William Leeb, Eitan Levin, and Amit Singer, "Toward single particle reconstruction without particle picking: breaking the detection limit," *arXiv preprint arXiv:1810.00226*, 2018.

[7] Richard Henderson, "The potential and limitations of neutrons, electrons and X-rays for atomic resolution microscopy of unstained biological molecules," *Quarterly Reviews of Biophysics*, vol. 28, no. 2, pp. 171–193, 1995.

[8] Eva Nogales, "The development of cryo-EM into a mainstream structural biology technique," *Nature methods*, vol. 13, no. 1, pp. 24–27, 2016.

[9] Xiao-Chen Bai, Greg McMullan, and Sjors HW Scheres, "How cryo-EM is revolutionizing structural biology," *Trends in Biochemical Sciences*, vol. 40, no. 1, pp. 49–57, 2015.

[10] Joachim Frank, *Three-dimensional electron microscopy of macromolecular assemblies: visualization of biological molecules in their native state*, Oxford University Press, 2006.

[11] Tamir Bendory, Alberto Bartesaghi, and Amit Singer, "Single-particle cryo-electron microscopy: Mathematical theory, computational challenges, and opportunities," *IEEE Signal Processing Magazine*, vol. 37, no. 2, pp. 58–76, 2020.

[12] Amit Singer and Fred J Sigworth, "Computational methods for single-particle electron cryomicroscopy," *Annual Review of Biomedical Data Science*, vol. 3, pp. 163–190, 2020.

[13] Sjors HW Scheres, "RELION: implementation of a Bayesian approach to cryo-EM structure determination," *Journal of Structural Biology*, vol. 180, no. 3, pp. 519–530, 2012.

[14] Ali Punjani, John L Rubinstein, David J Fleet, and Marcus A Brubaker, "cryoSPARC: algorithms for rapid unsupervised cryo-EM structure determination," *Nature methods*, vol. 14, no. 3, pp. 290–296, 2017.

[15] Cecilia Aguerrebere, Mauricio Delbracio, Alberto Bartesaghi, and Guillermo Sapiro, "Fundamental limits in multi-image alignment," *IEEE Transactions on Signal Processing*, vol. 64, no. 21, pp. 5707–5722, 2016.

[16] Edoardo D'Imprima and Werner Kühlbrandt, "Current limitations to high-resolution structure determination by single-particle cryoEM," *Quarterly Reviews of Biophysics*, vol. 54, 2021.

[17] Zvi Kam, "The reconstruction of structure from electron micrographs of randomly oriented particles," *Journal of Theoretical Biology*, vol. 82, no. 1, pp. 15–39, 1980.

[18] Tejal Bhamre, Teng Zhang, and Amit Singer, "Orthogonal matrix retrieval in cryo-electron microscopy," in *2015 IEEE 12th International Symposium on Biomedical Imaging (ISBI)*. IEEE, 2015, pp. 1048–1052.

[19] Tejal Bhamre, Teng Zhang, and Amit Singer, "Anisotropic twicing for single particle reconstruction using autocorrelation analysis," *arXiv preprint arXiv:1704.07969*, 2017.

[20] Eitan Levin, Tamir Bendory, Nicolas Boumal, Joe Kileel, and Amit Singer, "3D ab initio modeling in cryo-EM by autocorrelation analysis," in *2018 IEEE 15th International Symposium on Biomedical Imaging (ISBI 2018)*. IEEE, 2018, pp. 1569–1573.

[21] Lars Peter Hansen, "Large sample properties of generalized method of moments estimators," *Econometrica*, vol. 50, no. 4, pp. 1029, 1982.

[22] Jeffrey M Wooldridge, "Applications of generalized method of moments estimation," *Journal of Economic perspectives*, vol. 15, no. 4, pp. 87–100, 2001.

[23] Saeed Akbar, Jannine Poletti-Hughes, Ramadan El-Faitouri, and Syed Zulfiqar Ali Shah, "More on the relationship between corporate governance and firm performance in the uk: Evidence from the application of generalized method of moments estimation," *Research in International Business and Finance*, vol. 38, pp. 417–429, 2016.

[24] Jianqing Fan and Yiqiao Zhong, "Optimal subspace estimation using overidentifying vectors via generalized method of moments," *arXiv preprint arXiv:1805.02826*, 2018.

[25] David Roodman, "How to do xtabond2: An introduction to difference and system GMM in stata," *The stata journal*, vol. 9, no. 1, pp. 86–136, 2009.

[26] Asaf Abas, Tamir Bendory, and Nir Sharon, "The generalized method of moments for multi-reference alignment," *arXiv preprint arXiv:2103.02215*, 2021.

[27] Robert De Jong and Chirok Han, "The properties of lp-GMM estimators," *Econometric Theory*, vol. 18, no. 2, pp. 491–504, 2002.

[28] Robert Beinert and Gerlind Plonka, "Enforcing uniqueness in one-dimensional phase retrieval by additional signal information in time domain," *Applied and Computational Harmonic Analysis*, vol. 45, no. 3, pp. 505–525, 2018.

[29] Tamir Bendory, Robert Beinert, and Yonina C Eldar, "Fourier phase retrieval: Uniqueness and algorithms," in *Compressed Sensing and its Applications*, pp. 55–91. Springer, 2017.

[30] Alastair R Hall, *Generalized method of moments*, Oxford university press, 2005.

[31] Richard Blundell and Stephen Bond, "GMM estimation with persistent panel data: an application to production functions," *Econometric reviews*, vol. 19, no. 3, pp. 321–340, 2000.

[32] Fred J Sigworth, "A maximum-likelihood approach to single-particle image refinement," *Journal of structural biology*, vol. 122, no. 3, pp. 328–339, 1998.

[33] Emmanuel Abbe, Tamir Bendory, William Leeb, João M Pereira, Nir Sharon, and Amit Singer, "Multireference alignment is easier with an aperiodic translation distribution," *IEEE Transactions on Information Theory*, vol. 65, no. 6, pp. 3565–3584, 2018.

[34] Amelia Perry, Jonathan Weed, Afonso S Bandeira, Philippe Rigollet, and Amit Singer, "The sample complexity of multireference alignment," *SIAM Journal on Mathematics of Data Science*, vol. 1, no. 3, pp. 497–517, 2019.